THE JOURNAL OF COMPARATIVE NEUROLOGY 437:79–90 (2001)

Neuromodulator Content of Hamster Intergeniculate Leaflet Neurons and Their Projection to the Suprachiasmatic Nucleus or Visual Midbrain

LAWRENCE P. MORIN[1,2]* AND JANE H. BLANCHARD[1]
[1]Department of Psychiatry, State University of New York, Stony Brook, New York 11794
[2]Program in Neurobiology and Behavior, State University of New York, Stony Brook, New York 11794

ABSTRACT

The intergeniculate leaflet (IGL) of the lateral geniculate complex has widespread, bilateral, and reciprocal connections with nuclei in the subcortical visual shell. Its function is poorly understood with respect to its role in visual processing. The most well-known IGL projection, and the only one with a clear function, is the geniculohypothalamic tract (GHT) that terminates in the suprachiasmatic nucleus (SCN), site of the primary circadian clock. The hamster GHT is derived, in part, from IGL neurons containing neuropeptide Y and enkephalin. IGL neurons containing these peptides also project to the pretectal region. The present studies used a combination of immunohistochemical, lesion, and retrograde tracing techniques to study neuron types in the IGL and their projections to hamster SCN and pretectum. Two additional neuromodulators, γ-aminobutyric acid (GABA) and neurotensin, are shown to be present in IGL neurons. The GABA- and neurotensin-immunoreactive neurons project to the SCN with terminal field patterns very similar to those for neuropeptide Y and enkephalin. IGL neurons of all four types also send projections to the pretectum, but rarely do individual cells project to both the SCN and the pretectum. Nearly all neurotensin is colocalized with neuropeptide Y in IGL neurons, although about half of the neuropeptide Y cells do not contain neurotensin. Otherwise, the extent to which the four neuromodulators are colocalized varies from 6% to 54%. Nearly every SCN neuron appears to contain GABA. In the IGL, the majority of cells studied are not identifiable by GABA immunoreactivity. Putative functions of the various neuromodulator projections from the IGL to pretectum or SCN are discussed. J. Comp. Neurol. 437:79–90, 2001.

Indexing terms: tract tracing; circadian; pretectum

The intergeniculate leaflet (IGL) was described originally as a small division intercalated between the dorsal lateral geniculate (DLG) and the ventral lateral geniculate (VLG) nuclei of the visual thalamus (Hickey and Spear, 1976). The IGL receives direct retinal projections (Hickey and Spear, 1976; Morin et al., 1992; Pickard, 1985) and processes photic information (Zhang and Rusak, 1989). Efferents of the IGL provide the hypothalamic suprachiasmatic nucleus (SCN), site of the primary circadian clock, with one of its three major input pathways (Morin, 1994). This geniculohypothalamic tract (GHT) originates exclusively in the IGL (Morin and Blanchard, 1995) and has been characterized in several rodents by the neuropeptide Y (NPY) of its neurons (Card and Moore, 1982; Harrington et al., 1985, 1987; Laemle et al., 1993; Smale et al., 1991; Goel et al., 1999; Smale and Boverhof, 1999). In the rat, most GHT neurons have been reported to contain γ-aminobutyric acid (GABA; Moore and Speh, 1993; Moore and Card, 1994). In the hamster, about 20% of the neurons in the GHT contain enkephalin (ENK) compared with 65 % that contain NPY, and about 50% of the neurons of each neuromodulator type contain the

Grant sponsor: NINDS; Grant number: NS22168.

*Correspondence to: Dr. Lawrence P. Morin, Ph.D., Department of Psychiatry, Health Science Center, State University of New York, Stony Brook, NY 11794-8101. E-mail: lmorin@epo.som.sunysb.edu

Received 20 October 2000; Revised 12 March 2001; Accepted 23 May 2001

other peptide (Morin and Blanchard, 1995). About 57% of hamster IGL neurons have not yet been associated with an identifiable neuromodulator, although preliminary evidence suggests that some contain GABA (Morin and Blanchard, 1998a). In addition, unpublished work from this laboratory has indicated that neurotensin (NT) is a fourth neuromodulator present in IGL neurons. With respect to function, the IGL has been found to modulate circadian period response to constant light (Pickard et al., 1987), entrainment to a skeleton photoperiod (Edelstein and Amir, 1999), entrainment to a short day photoperiod (Johnson et al., 1989), magnitude of phase response to light (Pickard et al., 1987), and rate of reentrainment (Johnson et al., 1989), and it is necessary for phase response to benzodiazepine or to stimulation from running in a novel wheel (Johnson et al., 1988; Janik and Mrosovsky, 1994; Wickland and Turek, 1994). Release of NPY from the GHT into the SCN is thought to be essential for regulating phase response to triazolam or novel wheel running (Albers and Ferris, 1984; Albers et al., 1984; Johnson et al., 1988; Biello et al., 1994).

The IGL may be a major integrator of nonimage-forming subcortical visual information given its widespread, bilateral, frequently reciprocal connections with nuclei of the subcortical visual shell (Morin and Blanchard, 1998b). We previously identified an IGL projection to the pretectum containing the neuromodulator, NPY, and a second contains ENK (Morin and Blanchard, 1995; Morin and Blanchard, 1997). One target of the pretectal projections is the posterior limitans nucleus (PLi). In addition, large numbers of fibers traverse the anterior pretectal nucleus (APT), terminating in or around the olivary pretectal nucleus (OPT).

The presence of distinct pathways, one to the pretectum and the other to the SCN, containing the same two neuromodulators suggested the possibility that NPY and ENK neurons in the IGL may bifurcate and project to both targets. Therefore, the present study was initiated, using retrograde tracers simultaneously applied to the SCN and pretectum, to determine whether individual NPY or ENK neurons provide efferent projections to both basal hypothalamus and dorsal midbrain. During the course of this investigation, we uncovered both NT and GABA neurons in the hamster IGL (Morin and Blanchard, 1999a). Their distributions and projections to SCN and pretectum also are described. Furthermore, we have determined the extent to which the four neuromodulators are colocalized in individual neurons projecting to either visual midbrain or SCN. Portions of these data were presented at the 1999 Society for Neuroscience meeting.

Abbreviations

3, 3V	third ventricle
AH	anterior hypothalamic nucleus
APT	anterior pretectal nucleus
CP	cerebral peduncle
CPT	commissural pretectal area
DLG	dorsal lateral geniculate nucleus
fr	fasciculus retroflexus
IGL	intergeniculate leaflet
LH	lateral hypothalamic nucleus
LP	lateral posterior thalamic nucleus
LTN	lateral terminal nucleus
MCPC	magnocellular nucleus of the posterior commissure
MG	medial geniculate nucleus
MPT	medial pretectal nucleus
NOT	nucleus of the optic tract
OPT	olivary pretectal nucleus
ot	optic tract
Pa	paraventricular hypothalamic nucleus
pc	posterior commissure
PLi, Pli	posterior limitans nucleus
PPT	posterior pretectal nucleus
pr	pineal recess
PrC	precommissural nucleus
SCN	suprachiasmatic nucleus
sox	supraoptic commissure
VLG	ventral lateral geniculate nucleus
ZI	zona incerta

MATERIALS AND METHODS

Adult male Golden hamsters (Charles River-Lakeview) were maintained in a 14-hour light:10-hour dark photoperiod with free access to Purina rodent chow and water. All animals were killed for anatomical purposes during the middle hours of daylight. All animals used for stereotaxic injections weighed about 120–130 g. These and the animals used for terminal histological procedures were deeply anesthetized with sodium pentobarbital (Anpro Pharmaceutical, Arcadia, CA; 100 mg/kg body weight). Procedures involving animal use were performed in accordance with approval by the university Institutional Animal Care and Use Committee and with National Institutes of Health guidelines.

Surgical procedures

A few animals (n = 7) were given N-methyl-DL-aspartic acid (NMDA; M-2137; Sigma, St. Louis, MO; 0.6 μl of 0.2 M NMDA in saline) neurotoxic lesions of the IGL. Injections were stereotaxically placed with a Hamilton syringe bilaterally and 1 week apart. Two to 3 weeks after the second injection, each animal was deeply anesthetized with pentobarbital (as described above), perfused, and its brain was taken for NPY and NT immunohistochemistry.

Other animals were placed in a stereotaxic instrument and given two tracer injections by iontophoresis using a Stoelting Precision Current Source and glass micropipettes (tip diameter, about 20 μm). One injection, as a matter of standard procedure in our laboratory, was a mixture of cholera toxin β fragment (CT-B; product 104; List Biological Laboratories, Inc., Campbell, CA; initially dissolved in distilled water) and *Phaseolus vulgaris*-leucoagglutinin (PHAL; Vector Laboratories, Burlingame, CA; initially dissolved in sodium phosphate-buffered saline, pH 7.2) that yields a final concentration of 1 % CT-B and 1.25% PHAL (Coolen and Wood, 1998; Morin and Blanchard, 1999b). The CT-B/PHAL combination was injected unilaterally into the SCN (6 μA pulsed 7 seconds on and 7 seconds off for about 6–10 minutes). The second injection was FluoroGold (FG; 4% in saline; Fluorochrome, Inc., Englewood, CO), which was injected unilaterally into the pretectum (5 μA pulsed 7 seconds on and 7 seconds off for 5 minutes). The PHAL data are not reported as part of this paper.

Stereotaxic coordinates for the IGL, SCN, and pretectum were those published previously (Morin and Wood, 2001). The pretectal sites were intended to place the injection in the general vicinity of the olivary pretectal nucleus (OPT) with no attempt to achieve the localization specificity we have reported previously. After the 3–7 days allowed for tracer transport, each animal was reanesthe-

tized with pentobarbital, placed in a stereotaxic instrument, and administered bilateral injections of colchicine (100 μg/5 μl saline per lateral ventricle). Twenty-four to 48 hours after the colchicine, animals were deeply anesthetized with pentobarbital (as described above) and perfused transcardially with physiological saline, pH 6.5, followed by 4% paraformaldehyde in 0.1 M phosphate buffer, pH 7.4, with 0.01 M sodium m-periodate and 0.075 lysine added (McLean and Nakane, 1974).

Each brain was removed, postfixed for 1 hour, cryoprotected in a series of sucrose solutions to 30% sucrose in phosphate buffer, then frozen, and serially sectioned (30 μm) in the coronal plane. Four series of sections were collected in 0.01 M phosphate-buffered saline (PBS), pH 7.2, with 0.05% sodium azide. All immunohistochemical reactions were performed using free-floating sections. Immunoperoxidase reactions were done using the avidin-biotin complex (ABC) technique (Elite kit; Vector Laboratories) and diaminobenzidine as the chromogen.

Tissue sections were incubated with the antisera at 4°C for 36–72 hours. Double immunofluorescent staining was performed using a mixture of two primary antisera, including goat anti-CT-B (1:25,000; List Biological Laboratories) and one of the following: rabbit anti-NPY (1:1,000; Peninsula Laboratories, Belmont, CA), sheep anti-NPY (1:5,000; Chemicon International, Temecula, CA), rabbit anti-TN (1:5,000; Oncogene Research Products, Cambridge, MA), mouse monoclonal anti-met/leu-enkephalin (1:200; Chemicon International), or guinea pig anti-GABA (1:1,000; ProtosBiotech Corp., New York, NY). Specificity of the NPY and ENK antisera has been established previously in hamsters (Morin et al., 1992), and CT-B has been used successfully as a retrograde tracer in hamsters (Morin and Blanchard, 1995, 1998b). Specificity of the NT antiserum was established by preabsorption with an excess of peptide (10 μg peptide/ml 0.01 M PBS, pH 7.2). Specificity of the GABA antiserum was determined by room temperature preabsorption of antiserum for 1 hour with 10 μM GABA conjugate solution. The blocking solution was made by mixing 10 mg/ml bovine serum albumin and 10 mM GABA in 0.01 M sodium phosphate buffer, pH 7.4, to a volume of 2 ml. To this was added sufficient glutaraldehyde to yield a 0.1% final concentration. The mixture was incubated on ice for 10 minutes, then dialyzed overnight against 100 mM Tris HCl buffer, pH 7.4, yielding an expected concentration of approximately 1 mM. Examination of the IGL and SCN revealed normal reaction product without preabsorption with peptide, but complete lack of immunoreactivity after the preabsorption step.

After several washes in PBS, pH 7.2, the sections used for fluorescence immunohistochemistry were incubated for 1–2 hours at room temperature in a mixture of secondary antisera that included a Texas red-conjugated donkey anti-goat immunoglobulin G (IgG; 1:50; Jackson ImmunoResearch, West Grove, PA) to label the CT-B and a biotinylated donkey anti-rabbit, mouse, sheep, or guinea pig IgG (1:250; Jackson ImmunoResearch). The final incubation was in streptavidin-conjugated Alexa 488 (1:200; Molecular Probes, Eugene, OR) to visualize the NPY, NT, ENK, or GABA immunoreactivity. The fluorescent material was mounted on gelatin-subbed slides from 0.01 M PBS, pH 7.2; dried overnight; and coverslipped with glass on Krystalon.

A Nikon Optiphot microscope (Tokyo, Japan) equipped for epifluorescence was used to identify Texas red-labeled neurons after an SCN injection of CT-B and FG-containing cells retrogradely labeled after an injection into the pretectum. Alexa 488 allowed fluorescent identification of immunoreactivity for NPY, ENK, NT, or GABA. Alexa 488 and Texas red were viewed using Nikon filters B-1A (470–490 nm excitation wavelengths) and G-1B (546 nm excitation wavelength), respectively. FG was viewed using the Nikon filter UV-1A (365 nm excitation wavelength). Cell counts of fluorescently labeled neurons were made according to criteria previously established (Morin and Blanchard, 1995). The total number of cells per brain was obtained from the raw counts of an entire tissue series through the IGL (usually 12 sections). Counts are uncorrected and are not intended to represent absolute numbers of cells. Moreover, accuracy of counts are subject to variation related to the time of day at perfusion as well as the effectiveness of colchicine treatment. All photomicrographs are digital images that were obtained using a Sound Vision SVMicro CM65 digital camera or were converted with a Hewlett-Packard digital scanner (5370C; Corvallis, OR) and software from 35-mm camera photomicrographic prints. A few of the images were modified digitally using Corel PhotoPaint 9 software to enhance contrast.

RESULTS

Peptide content of IGL neurons

NPY and ENK. NPY-immunoreactive (-IR) and ENK-IR neurons are scattered throughout the entire IGL. Their presence in the hamster IGL has been amply reported previously (Harrington et al., 1985, 1987; Morin et al., 1992; Morin and Blanchard, 1995, 1997).

NT. NT-IR neurons are distributed throughout the IGL (Figs. 1A, 2), the only location in the geniculate complex in which NT-IR neurons are found. This pattern is similar to what has been observed for NPY-IR neurons, including the presence of cells in the rostral and ventromedial IGL (Fig. 2A,D, respectively). The SCN contains an extensive, NT-IR terminal plexus (Fig. 1C) that is similar in its distribution characteristics to that described previously for NPY immunoreactivity (Fig. 1E) and ENK immunoreactivity (Morin et al., 1992). No NT-IR neurons were detected in the hamster SCN. Large neurotoxic lesions of the lateral geniculate region destroyed nearly all NT-IR neurons in the IGL. Sections through the IGL of a lesioned brain typically had no visible NT-IR neurons (Fig. 1B). In this animal, the adjacent section revealed the only two NT-IR neurons remaining in the lateral geniculate region (Fig. 1B′′). The SCN in this case was almost completely devoid of both the NT-IR (Fig. 1D) and NPY-IR (Fig. 1F) terminal fields. The loss of the NPY-IR terminal field in the SCN after NMDA lesions of the geniculate region is consistent with previous observations (Johnson et al., 1988). A pathway of fine, NT-IR fibers in the superior thalamic radiation extends between the pretectum and the IGL (Fig. 3). In particular, there is an NT-IR terminal plexus in the PLi as well as in the more medial pretectum, especially the OPT. A few fibers can be seen traversing the dorsal APT, apparently without terminating in it. No NT-IR neurons were evident in the pretectum. Neurotoxic lesions of the IGL eliminated virtually all of

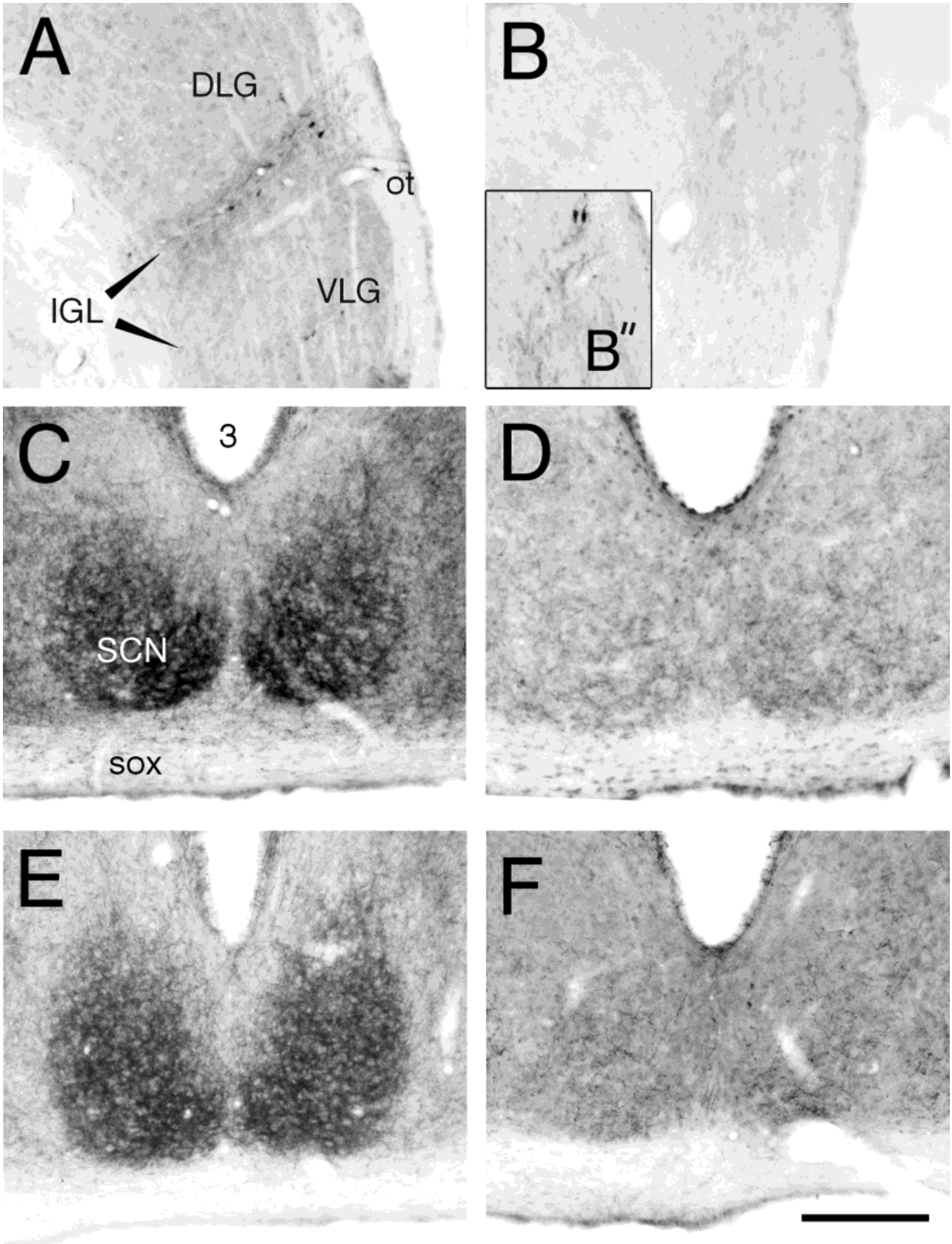

Fig. 1. Neurotensin (NT) immunoreactivity in the hamster intergeniculate leaflet (IGL) and SCN (suprachiasmatic nucleus). **A:** Normal distribution of NT-immunoreactive (NT-IR) neurons in the hamster IGL at a level equivalent to that shown in Figure 2D. **B:** Typical absence of NT-IR neurons in the IGL after an excitotoxic lesion. **B″:** In the tissue section adjacent to that shown in B, two NT-IR neurons are evident. These are the only neurons visible on this side of the brain in this animal. **C:** Normal NT-IR terminal plexus through the middle of the hamster SCN. **D:** Vastly reduced NT-IR terminal field in the SCN of the animal whose IGL is shown in B after a nearly complete bilateral lesion. **E:** Normal neuropeptide Y (NPY)-IR terminal plexus in the hamster SCN. **F:** Reduced NPY-IR terminal plexus in the IGL-lesioned animal. E and F are sections adjacent to C and D, respectively. For other abbreviations, see list. Scale bar = 200 μm.

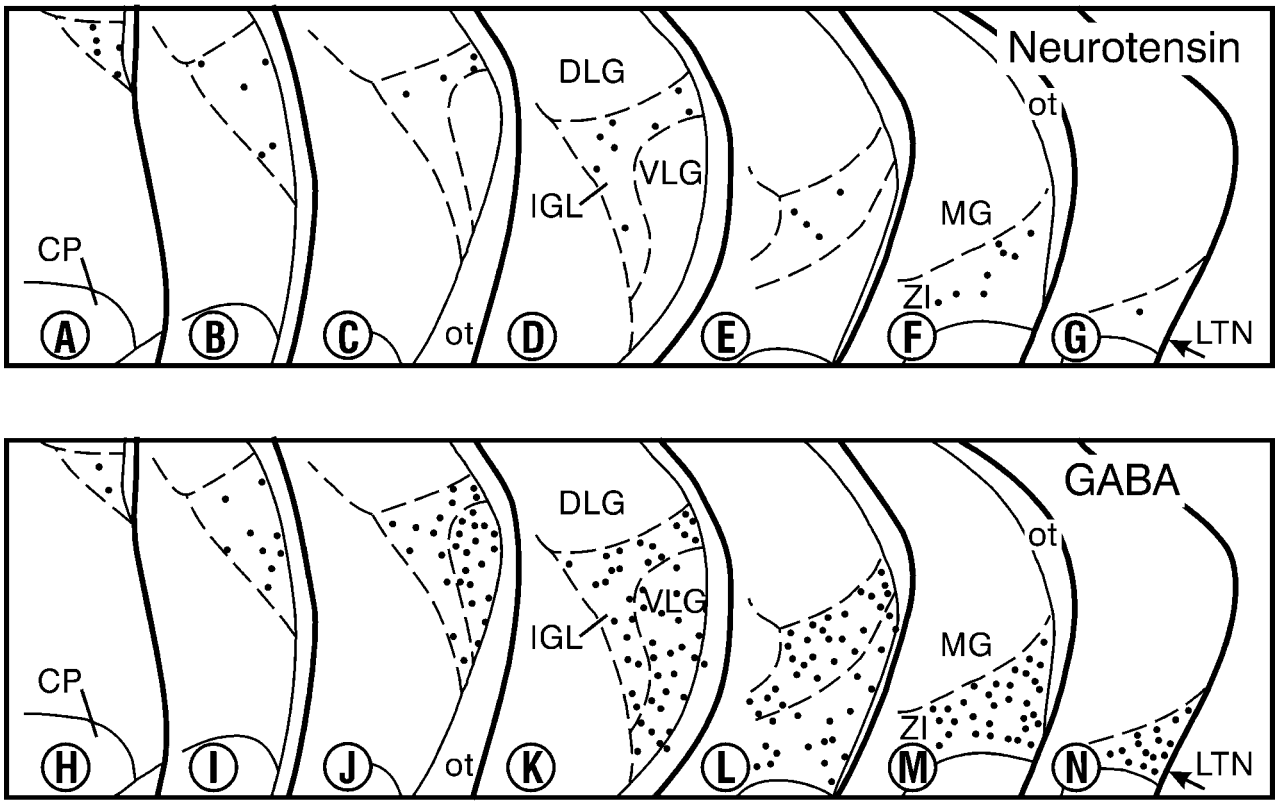

Fig. 2. **A–G:** Distribution of NT-IR neurons in the IGL of a normal hamster. **H–N:** Distribution of γ-aminobutyric acid (GABA)-IR neurons in the IGL and ventral lateral geniculate nucleus (VLG) of a normal hamster. Schematic sections are separated by about 210 μm. The figure is not meant to imply that GABA-IR neurons are not found elsewhere; there are such cells scattered in the dorsal lateral geniculate nucleus (DLG) and in areas medial to the IGL. For other abbreviations, see list.

the NT-IR terminal field within the pretectum (Fig. 3B). Residual pretectal-afferent NT-IR fibers appear to arrive from medial locations.

GABA. Moderately large numbers of GABA-IR neurons are distributed throughout the IGL (Figs. 2H–N, 4A). GABA-IR neurons are present throughout the lateral geniculate complex and are particularly evident in the ventral lateral geniculate nucleus. The pattern of GABA-IR neurons in the IGL is similar to that observed for NPY-IR neurons. The SCN is virtually filled with GABA-IR neurons and processes (Fig. 4B). Consequently, a presumptive IGL GABAergic projection to the SCN is not easily visualized using GABA immunohistochemistry.

Colocalization of NT, ENK, NPY, and GABA. All four neuromodulators are colocalized to some extent in IGL neurons (Table 1, Fig. 5). There are more GABA-IR neurons in the IGL than any of the other cell types, although relatively small percentages (7–9%) colocalize with one of the other peptides. The most obvious colocalization of peptides within one class of IGL neurons occurs with 98% of NT-IR neurons that also are immunoreactive to NPY. However, about half of the NPY-IR neurons do not contain NT-IR. Previously, we found that about 50% of ENK-IR or NPY-IR neurons contain the other peptide (Morin and Blanchard, 1995). The larger numbers of ENK-IR neurons found in the prior study serve to reinforce the point that the cell counts based on fluorescence microscopy should be considered relative rather than absolute. The 1995 investigation also showed that immunohistofluorescence methods detected only about 61% and 76% of NPY-IR and ENK-IR cells, respectively, that were found using the ABC technique. Regardless of the histological method used to identify the cell type, neither GABA-IR nor ENK-IR cell counts are possible without the successful use of colchicine pretreatment.

Projections of IGL to pretectum and SCN

A total of 21 animals received dual injections and successful tissue processing that enabled labeled cell evaluation for both tracers and one peptide.

Pretectal injections. On average, 87 ± 16 labeled neurons were counted in the combined ipsilateral and contralateral IGL (regardless of the pretectal injection site), with about 71% found in the ipsilateral nucleus after FG injections into the pretectum (Fig. 6A–F). Double-label analysis revealed that only a small percent of IGL neurons projecting to the pretectal region were immunoreactive for NPY, ENK, NT, or GABA (Table 2).

Variability in the numbers of FG-labeled IGL neurons appears to be related to the injection site (Table 3). For example, the pipette tip for Case 98-36 was in the lateral posterior thalamic nucleus, just lateral to the PLi but including the dorsal PLi. This brain had only six FG-labeled neurons evident in the IGL. This result is consistent with previous observations that the IGL does not

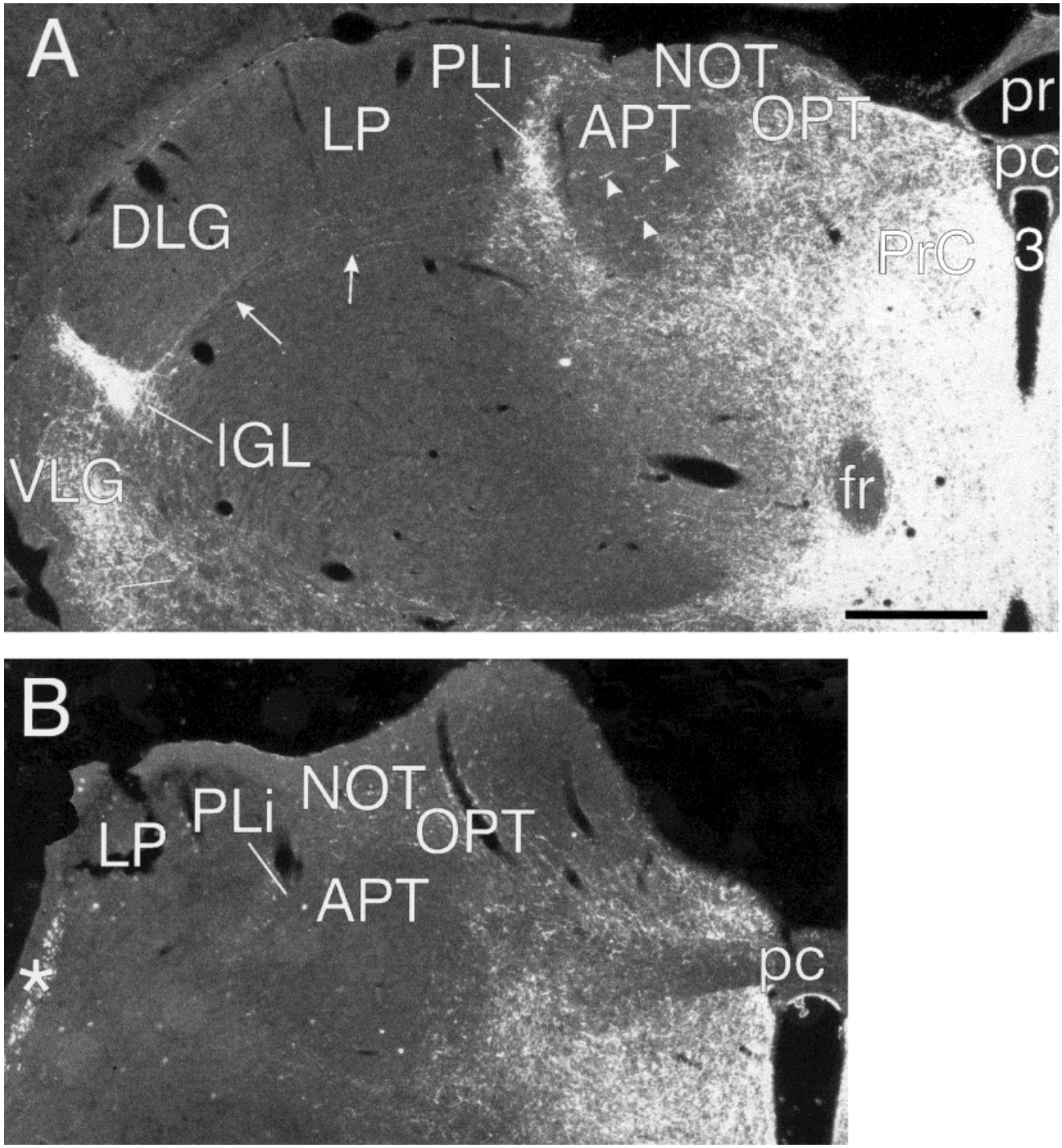

Fig. 3. Darkfield photomicrographs showing NT-IR fibers in the IGL and nuclei of the pretectum of a normal hamster (**A**) and a hamster that sustained bilateral neurotoxic lesions of the IGL (**B**). At the level shown, the IGL is not identifiable after the lesion. In A, arrowheads identify NT-IR fibers traversing the anterior pretectal nucleus (APT). Arrows indicate fine fibers in the superior thalamic radiation. The asterisk in B denotes a staining artifact. For other abbreviations, see list. Scale bar = 500 μm.

project to the lateral posterior nucleus (Morin and Blanchard, 1998b). In addition, the labeled neurons are overwhelmingly (94%) in the ipsilateral IGL after a PLi injection. Retrograde label injection into the OPT yielded fairly large numbers of IGL neurons that were labeled both ipsilaterally and contralaterally, although most (about 63%) were ipsilateral. Injections of FG into the commissural pretectal area (CPT) labeled an intermediate num-

ber of ipsilateral and contralateral IGL neurons, with the majority (74%) also in the ipsilateral IGL.

SCN injections. Injections were placed successfully in the SCN ipsilateral to the pretectal injection site in 19 of 21 cases (Fig. 6G–I). After retrograde CT-B tracer injection into one SCN, an average of 76 ± 6 labeled neurons were observed in the ipsilateral IGL, and 55 ± 6 neurons were observed in the contralateral IGL. Of the 19 brains with injections that did not span the midline, 18 had more retrogradely labeled neurons in the IGL ipsilateral to the injected SCN (these results are similar to those of Pickard, 1982). Approximately 50% of the CT-B-labeled IGL neurons were immunoreactive for NPY, 22% were immunoreactive for NT (Fig. 6A,B), 20% were immunoreactive for ENK, and 8% were immunoreactive for GABA (Table 2).

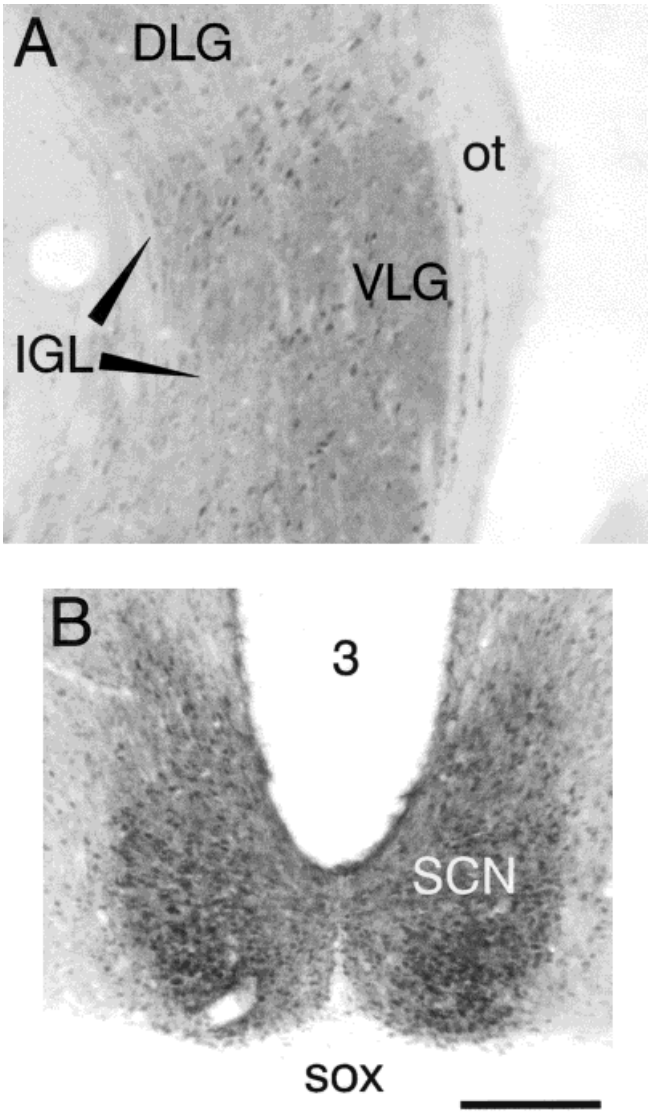

Fig. 4. Brightfield photomicrographs showing GABA-IR neurons in a section through the middle level of the hamster IGL (**A**) and in a section through the middle level of the hamster SCN (**B**). For abbreviations, see list. Scale bar = 200 μm.

There was scatter among injection sites in the SCN, although each injection encompassed a large portion of at least one nucleus. The resulting numbers of labeled IGL neurons were sufficiently variable to provoke an analysis of their relationship to the distance from brain midline to the actual injection site. The contralateral/ipsilateral disparity with respect to the number of CT-B-labeled neurons in each IGL was determined for each brain by calculating the ratio of labeled cells in the contralateral IGL to those in the ipsilateral IGL. Correlations were then examined between the distance measure, the disparity measure, and the sum of labeled neurons counted in both IGLs of each brain. The results show that greater distance to the midline from the SCN injection site is associated with higher ipsilateral/contralateral IGL cell count disparity [correlation coefficient (r) = 0.525; $P = 0.02$; Spearman test]. Larger distance also is associated with fewer CT-B-labeled neurons in the two IGLs (r = 0.574; $P = 0.01$). In addition, the number of labeled IGL cells inversely predicts the extent of contralateral versus ipsilateral IGL cell count disparity (r = − 0.495; $P = 0.03$).

SCN and pretectal injections. Very few neurons were found that projected to both the SCN and the pretectum (Fig. 7). Five of the 21 cases had 1 such cell each, and a 6th case had two positive CT-B/FG double-labeled cells. These comprised less than 0.5% of all CT-B- or FG-labeled IGL per brain (regardless of side relative to the injections). Three of the six cases involved injections into the OPT; two were into the PLi, and the injection that provided two double-labeled cells included both the CPT and the MPT. Triple-label fluorescence analysis did not identify any neurons that projected to both the SCN and the pretectum that also were immunoreactive for NPY, ENK, NT, or GABA.

DISCUSSION

The IGL was described originally as a small, thin lamination intercalated between the dorsal and ventral lateral geniculate nuclei (Hickey and Spear, 1976). It is now clear that the hamster IGL is a fairly large structure that

TABLE 1. Peptide-Immunoreactive Cells per Single Intergeniculate Leaflet and Extent of Localization of One Peptide With Another in Cells of the Intergeniculate Leaflet[1]

Peptide combination (no.)	Mean counted cells	Mean no. double-labeled cells	Colocalization	Colocalization
GABA/ENK (3)	355/44	24	GABA 7% with ENK	ENK 55% with GABA
NT/ENK (4)	81/44	19	NT 23% with ENK	ENK 43% with NT
NT/GABA (3)	106/425	32	NT 30% with GABA	GABA 8% with NT
NT/NPY (3)	58/106	57	NT 98% with NPY	NPY 54% with NT
GABA/NPY (3)	368/172	32	GABA 9% with NPY	NPY 19% with GABA
ENK/NPY (5)[a]	158/153	77	ENK 49% with NPY	NPY 51% with ENK

[1]GABA, γ-aminobutyric acid; ENK, enkephalin; NT, neurotensin; NPY, neuropeptide Y.
[a]Modified from (Morin and Blanchard, 1995).

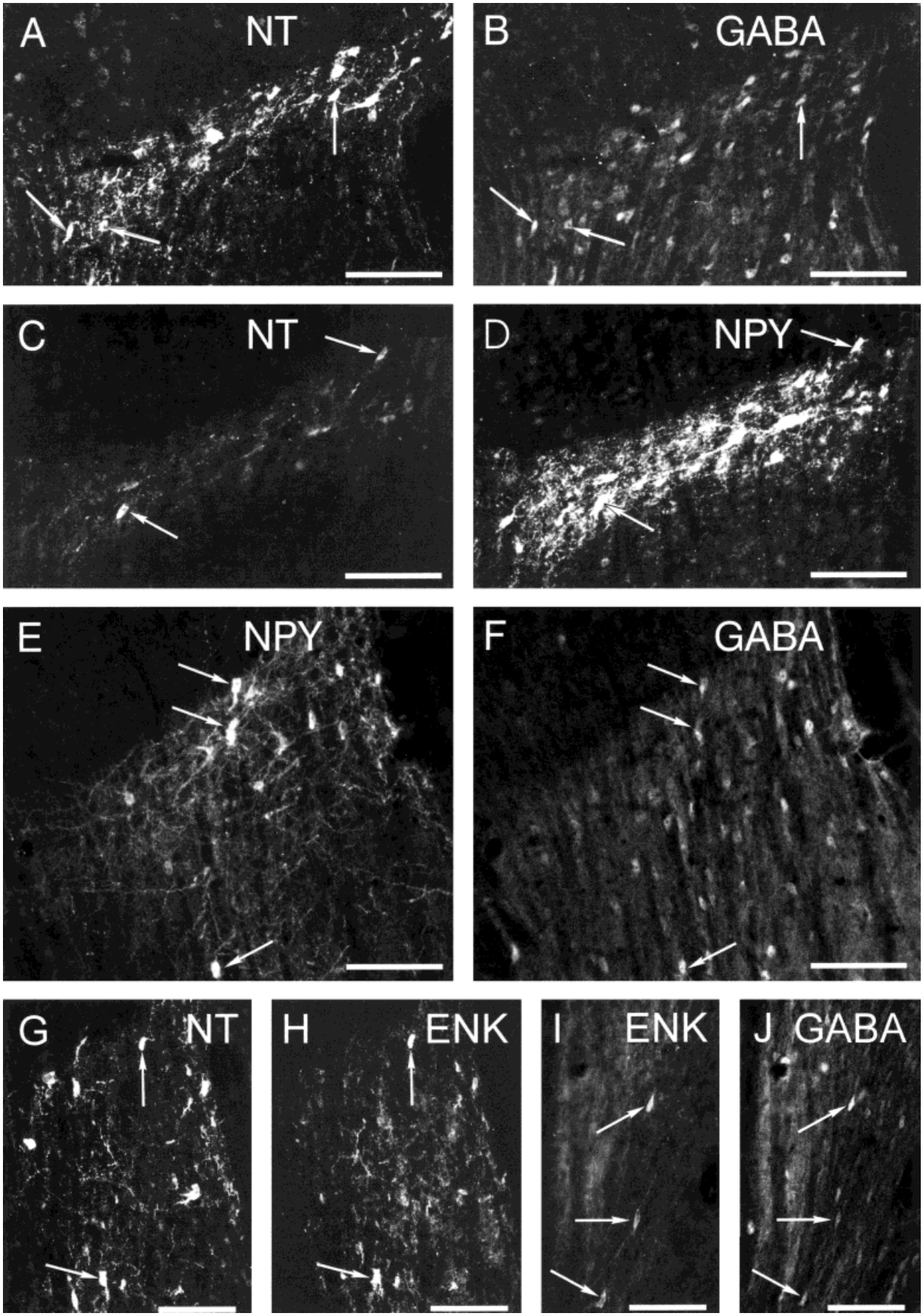

Fig. 5. Photomicrographs showing immunofluorescence of two co-localized peptides in neurons of the IGL: NT immunoreactivity (-IR) in neurons (**A**) that also contain GABA-IR (**B**); NT-IR in neurons (**C**) that also contain NPY-IR (**D**); NPY-IR in neurons (**E**) that also contain GABA-IR (**F**); NT-IR in neurons (**G**) that also contain enkephalin (ENK)-IR (**H**); and ENK-IR in neurons (**I**) that also contain GABA-IR (**J**). Colocalization of ENK- and NPY-IR (not shown) has been demonstrated previously (Morin and Blanchard, 1995). Scale bars = 100 μm.

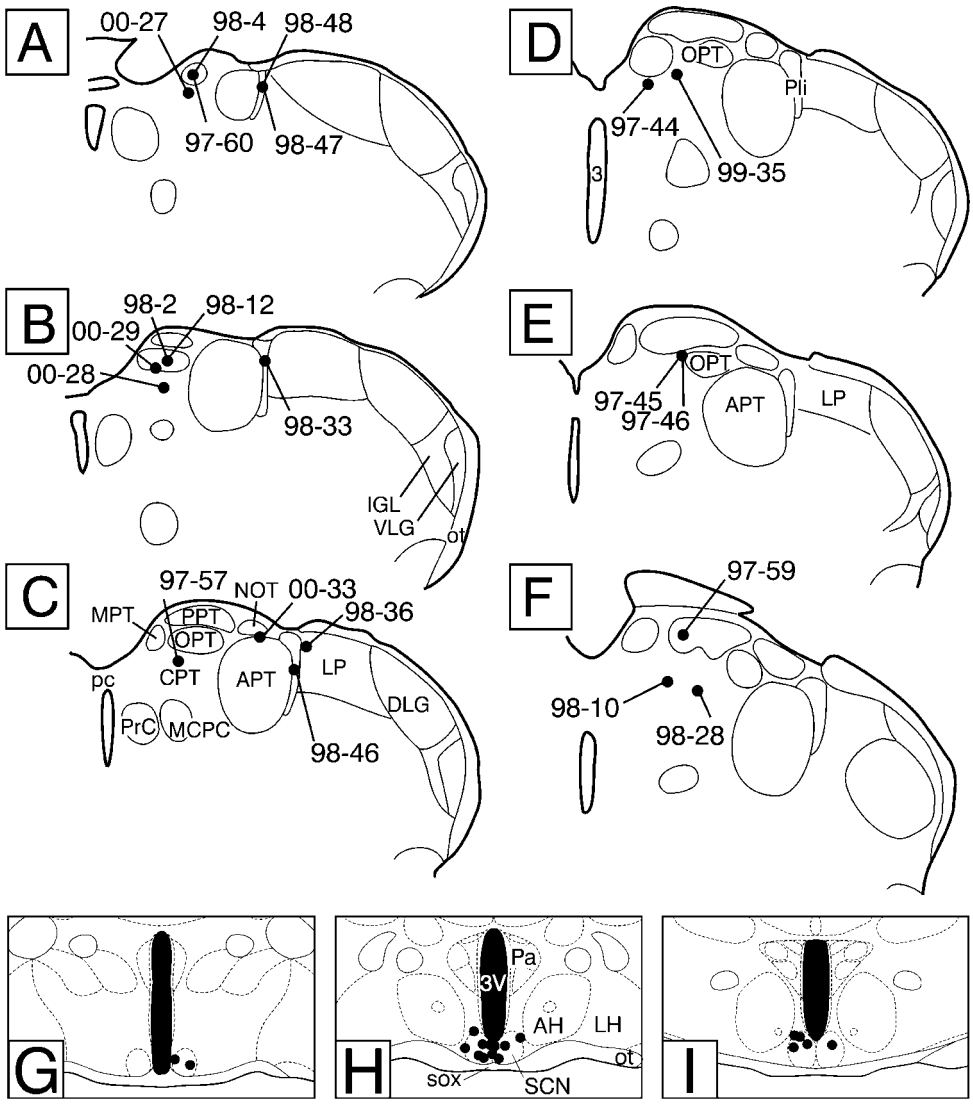

Fig. 6. Sites of FluoroGold (FG) injections placed in the pretectal area (**A–F**) and locations of cholera toxin subunit β (CT-B) injections aimed at the SCN (**G–I**). For abbreviations, see list.

TABLE 2. Extent of Peptide Colocalization in Intergeniculate Leaflet Neurons Retrogradely Labeled by Tracer Injected into the Pretectum or the Suprachiasmatic Nucleus

Injection site	Mean (±S.E.M.) IGL cells labeled by injection	% Retrogradely labeled cells with peptide/% of peptide cells with retrograde label[1]			
		NPY	ENK	NT	GABA
SCN	76 ± 6	50/20	20/20	22/35	8/3
Pretectum	87 ± 16	9/5	<1/<1	1/5	<1/1

[1]IGL, intergeniculate leaflet; NPY, neuropeptide Y; ENK, enkephalin; NT, neurotensin; GABA, γ-aminobutric acid.

encompasses regions previously considered parts of the VLG (Morin et al., 1992). Overall, the hamster IGL is about 2 mm long and exhibits marked changes in its coronal profile along its rostrocaudal axis. Early analysis of IGL connections emphasized those with the hypothalamic SCN and the contralateral IGL (Card and Moore, 1989). More recently, several investigators have noted the widespread efferent and afferent connections between the IGL, midbrain, diencephalon, and other cortical and subcortical forebrain areas (Horvath, 1998; Mikkelsen and Moller, 1990; Mikkelsen, 1990a,b, 1992; Morin and Blanchard, 1998b,1999b; Moore et al., 2000). The extent of such connections is consistent with the present understanding of IGL size.

GHT

The rodent SCN contains a dense, NPY-IR terminal plexus with cells of origin uniquely in the IGL (Card and Moore, 1989; Morin et al., 1992; Moore and Card, 1994; Morin and Blanchard, 1997). The NPY-IR neurons are scattered throughout the IGL, and their presence allows a straightforward approximation of IGL boundaries (Morin and Blanchard, 1995). However, the location of lateral geniculate neurons projecting to the SCN is a more robust criterion by which the IGL can be defined, because there are more neurons contributing to the GHT than there are NPY-IR cells (Morin et al., 1992; Morin and Blanchard, 1995; present data). This is particularly important in the hamster ventromedial IGL region (cf., Fig. 2C,D), where there is known to be a relative paucity of NPY-IR neurons but greater numbers of SCN-afferent cells. Prior to recognition of the IGL as a separate entity, this region was called the *dorsal lamina of the interior division of the VLG* and had cellular attributes described as similar to those in the leaflet region (Frost et al., 1979).

The present data reaffirm the use of GHT neurons to define the hamster IGL but augment the definition by demonstrating that substantial numbers of neurons in the GHT are immunoreactive to NT and GABA. Of these, the NT-IR neurons are particularly useful, because, like the NPY-IR cells (Morin et al., 1992; Morin and Blanchard, 1995), they also are found only in the IGL of the lateral geniculate complex. Indeed, the NT-IR neurons appear to comprise a 50% subset of the NPY-IR neurons to the extent that virtually all are also immunoreactive to both NT and NPY. The GABA-IR neurons, although they are abundant in the IGL, also are abundant in the adjacent geniculate nuclei. Similarly, ENK-IR neurons are common in the IGL but are present in larger numbers in the VLG (Morin and Blanchard, 1995). Many of those in the IGL contribute to the GHT, whereas those in the VLG do not. Other criteria that have contributed to the definition of the IGL include location of substance P-IR terminals, migration path of NPY-IR neurons in conjunction with the developmental origin and distribution of astrocytes, location of retinal afferents, and location of neurons projecting to contralateral subcortical visual nuclei (Morin et al., 1992; Botchkina and Morin, 1995; Morin and Blanchard, 1998b)

Indirect methods of calculation suggested that all rat IGL neurons contain GABA (Moore and Speh, 1993). The present data show that, at best, only about 50% of NT-, ENK-, or NPY-IR neurons in the IGL are also GABA-IR neurons. A preliminary analysis of hamster brain sections costained for Nissl substance and GABA immunoreactivity indicates that only about 50% of IGL neurons contain GABA (our unpublished data). More recent analysis of the rat IGL indicates that it is comprised of GABA, NPY, and ENK neurons plus a fourth type of neuron that contains a currently unknown neuromodulator (Moore and Card, 1994). The unknown neuromodulator is not NT, which is evident in rat SCN neurons, although not in the rat IGL (our unpublished data). The rat ENK neurons project to the contralateral IGL, and not to the SCN as in the hamster (Card and Moore, 1989; Morin et al., 1992; Morin and Blanchard, 1995). The present data show extensive colocalization of the four neuromodulators in IGL neurons. However, we presently are unable to perform the multiple-labeling procedures necessary to determine di-

TABLE 3. Mean Count of FluoroGold-Labeled Neurons in the Ipsilateral- or Contralateral Intergeniculate Leaflet after Label Injection into One or More Nuclei of the Pretectum

Injection site[1]				
CPT	OPT	PLi	OPT/PPT	CPT/MPT/OPT
56/10 (4)	106/55 (6)	33/2 (4)	28/11 (2)	94/58 (2)

[1]ipsilateral cells/contralateral cells (N) (no.). CPT, commisural pretectal nucleus; OPT, olivary pretectal nucleus; PLi, posterior limitans nucleus.

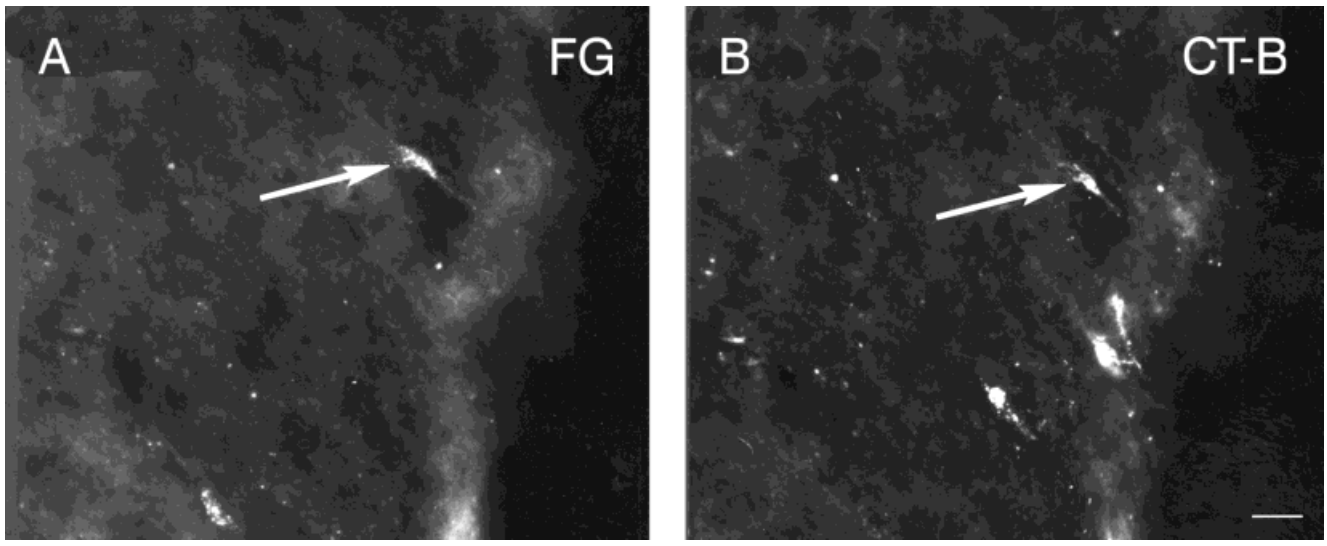

Fig. 7. Photomicrographs showing an IGL neuron labeled with FF after tracer injection into the pretectum (**A**) and labeled with CT-B immunofluorescence after a tracer injection into the SCN (**B**). Scale bar = 20 μm.

rectly whether the four neuron types account for all cells that project to the SCN or the pretectum.

Geniculopretectal tract

Until recently, there has been little known about connections between the IGL and the visual midbrain. The initial analysis revealed NPY and ENK fibers extending between the IGL and nuclei in the pretectum with terminal regions particularly evident in the PLi and the olivary pretectal nucleus (Morin and Blanchard, 1995). Tract-tracing methods have demonstrated further that the IGL both projects to and receives projections from essentially all midbrain nuclei in the subcortical visual system (Morin and Blanchard, 1998b). The present data reaffirm the existence of extensive pretectal IGL projections and further reveal that each of the four neuromodulators found in IGL neurons is represented by a small subset of IGL to pretectum projections. The data permit the additional conclusion that IGL neurons project more extensively to the OPT than to the PLi, consistent with previous observations (Morin and Blanchard, 1998b). An interesting feature concerning the IGL-pretectum interconnection is that NPY- and ENK-IR neurons are found in both the IGL and the OPT. The peptidergic projections from the IGL have been identified, as indicated above. It is possible, although undetermined at the present time, that OPT neurons containing the same peptides project to the IGL. In either case, it is not known whether the axons containing one peptide synapse on neurons with the same or different neuromodulator content.

Functional considerations

Function has been established only for the GHT. Loss of the GHT consequent to IGL lesion modifies the phase-response curve to light, reduces the rate of reentrainment to light, and eliminates phase response to benzodiazepine or locomotion-inducing stimuli. Electrical or chemical stimulation of the IGL can cause phase shifts described by a phase-response curve similar to that derived by direct application of NPY to the SCN. Finally, chemical blockade of NPY activity eliminates phase response to locomotion-inducing stimuli. Collectively, these studies indicate that activation of IGL neurons during the midsubjective day releases NPY from GHT terminals in the SCN. The NPY induces moderately large phase advances at that time and, during the early subjective night, induces small phase delays. The NPY is thought to exert its effects via modulation of period gene expression in circadian rhythm-generating neurons of the SCN (Maywood et al., 1999).

Functional evaluation of the ENK contribution to circadian rhythm regulation has just begun. Recent reports indicate that the δ-opioid receptor is distributed throughout the SCN (Byku et al., 2000). Furthermore, a δ-opioid receptor agonist is able to elicit circadian rhythm phase response with significant phase advances occurring mid-subjective day (Byku and Gannon, 2000). This suggests a degree of functional similarity to the NPY-type phase-response curve. However, there is no phase delay portion of the curve in response to the opioid agonist, and, because the agonist has been injected peripherally, the target of its rhythm-related activity is uncertain.

Functional evaluation of the GABAergic component of the GHT is more difficult, because most, if not all, neurons of the SCN also contain GABA (Moore and Speh, 1993; Decavel and van den Pol, 1990; present data; however, see Castel et al., 1997). Many of the SCN neurons have short GABAergic projections to neighboring cells (Buijs et al., 1994). Thus, any result consequent to GABA receptor manipulation in the SCN cannot exclude the possibility that the action is unrelated to GHT activity. To date, there have been no attempts to test function of the GABA component of the GHT by direct manipulation of the IGL. Nevertheless, GABA agonists act in the SCN to induce phase advances during the subjective day (Tominaga et al., 1994; Huhman et al., 1997; Bergeron et al., 1999).

There have been no published studies evaluating the possibility that NT participates in circadian rhythm regulation. However, NT receptors have been described on vasoactive intestinal polypeptide neurons and on serotonin axons in the rat SCN (François-Bellan et al., 1992).

With respect to the IGL projections to pretectum, no function has yet been established. The fact of robust bilaterality of both IGL efferents and afferents suggests that the IGL contributes to the regulation of motor systems that control symmetrical ocular movements (for review, see Morin and Blanchard, 1998b). The substrate of the circadian rhythm system recently has been expanded to include the visual midbrain (Marchant and Morin, 1999). In the absence of functional tectum or pretectum or of their connections with the IGL, benzodiazepine (but not novel wheel-induced locomotion) is unable to induce phase shifts in hamster circadian rhythmicity. To date, the specific brain nuclei, pathways, or direction of information flow necessary for response to benzodiazepine have not been discerned.

ACKNOWLEDGMENTS

We thank Ms. L. Pace for histological assistance.

LITERATURE CITED

Albers HE, Ferris CF. 1984. Neuropeptide Y: role in light-dark entrainment of hamster circadian rhythms. Neurosci Lett 50:163–168.

Albers HE, Ferris CF, Leeman SE, Goldman BD. 1984. Avian pancreatic polypeptide phase shifts hamster circadian rhythms when microinjected into the suprachiasmatic region. Science 223:833–835.

Bergeron HE, Danielson B, Biggs KR, Prosser RA. 1999. TTX blocks baclofen-induced phase shifts of the mammalian circadian pacemaker in vitro. Brain Res 841:193–196.

Biello SM, Janik D, Mrosovsky N. 1994. Neuropeptide Y and behaviorally induced phase shifts. Neuroscience 62:273–279.

Botchkina GI, Morin LP. 1995. Specialized neuronal and glial contributions to development of the hamster lateral geniculate complex and circadian visual system. J Neurosci 15:190–201.

Buijs RM, Hou Y-X, Shinn S, Renaud LP. 1994. Ultrastructural evidence for intra- and extranuclear projections of GABAergic neurons of the suprachiasmatic nucleus. J Comp Neurol 340:381–391.

Byku M, Gannon RL. 2000. SNC 80, a delta-opioid agonist, elicits phase advances in hamster circadian activity rhythms. Neuroreport 11:1449–1452.

Byku M, Legutko R, Gannon RL. 2000. Distribution of δ opioid receptor immunoreactivity in the hamster suprachiasmatic nucleus and intergeniculate leaflet. Brain Res 857:1–7.

Card JP, Moore RY. 1982. Ventral lateral geniculate nucleus efferents to the rat suprachiasmatic nucleus exhibit avian pancreatic polypeptide-like immunoreactivity. J Comp Neurol 206:390–396.

Card JP, Moore RY. 1989. Organization of lateral geniculate-hypothalamic connections in the rat. J Comp Neurol 284:135–147.

Castel M, Belenky M, Cohen S, Wagner S, Schwartz WJ. 1997. Light-induced c-Fos expression in the mouse suprachiasmatic nucleus: immunoelectron microscopy reveals co-localization in multiple cell types. Eur J Neurosci 9:1950–1960.

Coolen LM, Wood RI. 1998. Bidirectional connections of the medial amygdaloid nucleus in the Syrian hamster brain: simultaneous anterograde and retrograde tract tracing. J Comp Neurol 399:189–209.

Decavel C, van den Pol AN. 1990. GABA: a dominant neurotransmitter in the hypothalamus. J Comp Neurol 302:1019–1037.

Edelstein K, Amir S. 1999. The role of the intergeniculate leaflet in entrainment of circadian rhythms to a skeleton photoperiod. J Neurosci 19:372–380.

François-Bellan A-M, Bosler O, Tonon M-C, Lin-Tong W, Beaudet A. 1992. Association of neurotensin receptors with VIP-containing neurons and serotonin-containing axons in the suprachiasmatic nucleus of the rat. Synapse 10:282–290.

Frost DO, So K-F, Schneider GE. 1979. Postnatal development of retinal projections in Syrian hamsters: a study using autoradiographic and anterograde degeneration techniques. Neuroscience 4:1649–1677.

Goel N, Lee TM, Smale L. 1999. Suprachiasmatic nucleus and intergeniculate leaflet in the diurnal rodent *Octodon degus*: retinal projections and immunocytochemical characterization. Neuroscience 92:1491–1509.

Harrington ME, Nance DM, Rusak B. 1985. Neuropeptide Y immunoreactivity in the hamster geniculo-suprachiasmatic tract. Brain Res Bull 15:465–472.

Harrington ME, Nance DM, Rusak B. 1987. Double-labeling of neuropeptide Y-immunoreactive neurons which project from the geniculate to the suprachiasmatic nuclei. Brain Res 410:275–282.

Hickey TL, Spear PD. 1976. Retinogeniculate projections in hooded and albino rats: an autoradiographic study. Exp Brain Res 24:523–529.

Horvath TL. 1998. An alternate pathway for visual signal integration into the hypothalamo-pituitary axis: retinorecipient intergeniculate neurons project to various regions of the hypothalamus and innervate neuroendocrine cells including those producing dopamine. J Neurosci 18:1546–1558.

Huhman KL, Marvel CL, Gillespie CF, Mintz EM, Albers HE. 1997. Tetrodotoxin blocks NPY-induced but not muscimol-induced phase advances of wheel-running activity in Syrian hamsters. Brain Res 772: 176–180.

Janik D, Mrosovsky N. 1994. Intergeniculate leaflet lesions and behaviorally-induced shifts of circadian rhythms. Brain Res 651:174–182.

Johnson RF, Smale L, Moore RY, Morin LP. 1988. Lateral geniculate lesions block circadian phase shift responses to a benzodiazepine. Proc Natl Acad Sci USA 85:5301–5304.

Johnson RF, Moore RY, Morin LP. 1989. Lateral geniculate lesions alter activity rhythms in the hamster. Brain Res Bull. 22:411–422.

Laemle LK, Fugaro C, Bentley T. 1993. The geniculohypothalamic pathway in a congenitally anophthalmic mouse. Brain Res 618:352–357.

Marchant EG, Morin LP. 1999. The hamster circadian rhythm system includes nuclei of the subcortical visual shell. J Neurosci 19:10482–10493.

Maywood ES, Mrosovsky N, Field MD, Hastings MH. 1999. Rapid down-regulation of mammalian *Period* genes during behavioral resetting of the circadian clock. Proc Natl Acad Sci USA 96:15211–15216.

McLean IW, Nakane PK. 1974. Periodate-lysine-paraformaldehyde fixative: a new fixative for immunoelectron microscopy. J Histochem Cytochem 22:1077–1083.

Mikkelsen JD. 1990a. A neuronal projection from the lateral geniculate nucleus to the lateral hypothalamus of the rat demonstrated with *Phaseolus vulgaris*-leucoagglutinin tracing. Neurosci Lett 116:58–63.

Mikkelsen JD. 1990b. Projections from the lateral geniculate nucleus to the hypothalamus of the Mongolian gerbil (*Meriones unguiculatus*): an anterograde and retrograde tracing study. J Comp Neurol 299:493–508.

Mikkelsen JD. 1992. The organization of the crossed geniculogeniculate pathway of the rat: a *Phaseolus vulgaris*-leucoagglutinin study. Neuroscience 48:953–962.

Mikkelsen JD, Moller M. 1990. A direct neural projection from the intergeniculate leaflet of the lateral geniculate nucleus to the deep pineal gland of the rat, demonstrated with *Phaseolus vulgaris*-leucoagglutinin. Brain Res 520:342–346.

Moore RY, Card JP. 1994. Intergeniculate leaflet: an anatomically and functionally distinct subdivision of the lateral geniculate complex. J Comp Neurol 344:403–430.

Moore RY, Speh JC. 1993. GABA is the principal neurotransmitter of the circadian system. Neurosci Lett 150:112–116.

Moore RY, Weis R, Moga MM. 2000. Efferent projections of the intergeniculate leaflet and the ventral lateral geniculate nucleus in the hat. J Comp Neurol 420:398–418.

Morin LP. 1994. The circadian visual system. Brain Res Rev 67:102–127.

Morin LP, Blanchard JH. 1995. Organization of the hamster intergeniculate leaflet: NPY and ENK projections to the suprachiasmatic nucleus, intergeniculate leaflet and posterior limitans nucleus. Vis Neurosci 12:57–67.

Morin LP, Blanchard JH. 1997. Neuropeptide Y and enkephalin immunoreactivity in retinorecipient nuclei of the hamster pretectum and thalamus. Vis Neurosci 14:765–777.

Morin LP, Blanchard JH. 1998a. Distribution of GABA neurons and GABA/benzodiazepine receptor in the hamster circadian and subcortical visual systems. Soc Neurosci Abstr 24:1918.

Morin LP, Blanchard JH. 1998b. Interconnections among nuclei of the subcortical visual shell: the intergeniculate leaflet is a major constituent of the hamster subcortical visual system. J Comp Neurol 396:288–309.

Morin LP, Blanchard JH. 1999a. Neurotensin and NPY neurons in the hamster intergeniculate leaflet have similar projection patterns to the suprachiasmatic nucleus. Soc Neurosci Abstr 29:1133.

Morin LP, Blanchard JH. 1999b. Forebrain connections of the hamster intergeniculate leaflet: comparison with those of ventral lateral geniculate nucleus and retina. Vis Neurosci 16:1037–1054.

Morin LP, Wood RI. 2001. A stereotaxic atlas of the golden hamster brain. New York: Academic Press.

Morin LP, Blanchard JH, Moore RY. 1992. Intergeniculate leaflet and suprachiasmatic nucleus organization and connections in the hamster. Vis Neurosci 8:219–230.

Pickard GE. 1982. The afferent connections of the suprachiasmatic nucleus of the golden hamster with emphasis on the retinohypothalamic projection. J Comp Neurol 211:65–83.

Pickard GE. 1985. Bifurcating axons of retinal ganglion cells terminate in the hypothalamic suprachiasmatic nucleus and the intergeniculate leaflet of the thalamus. Neurosci Lett 55:211–217.

Pickard GE, Ralph MR, Menaker M. 1987. The intergeniculate leaflet partially mediates effects of light on circadian rhythms. J Biol Rhythms 2:35–56.

Smale L, Boverhof J. 1999. The suprachiasmatic nucleus and intergeniculate leaflet of *Arvicanthis niloticus*, a diurnal murid rodent from East Africa. J Comp Neurol 403:190–208.

Smale L, Blanchard JH, Moore RY, Morin LP. 1991. Immunocytochemical characterization of the suprachiasmatic nucleus and the intergeniculate leaflet in the diurnal ground squirrel, *Spermophilus lateralis*. Brain Res 563:77–86.

Tominaga K, Shibata S, Hamada T, Watanabe S. 1994. $GABA_A$ receptor agonist muscimol can reset the phase of neural activity rhythm in the rat suprachiasmatic nucleus in vitro. Neurosci Lett 166:81–84.

Wickland C, Turek FW. 1994. Lesions of the thalamic intergeniculate leaflet block activity- induced phase shifts in the circadian activity rhythm of the golden hamster. Brain Res 660:293–300.

Zhang DX, Rusak B. 1989. Photic sensitivity of geniculate neurons that project to the suprachiasmatic nuclei or the contralateral geniculate. Brain Res 504:161–164.